ORIGINAL ARTICLE

Investigating sustained attention in contextual threat using steady-state VEPs evoked by flickering video stimuli

Yannik Stegmann[1] | Marta Andreatta[1,2] | Paul Pauli[1,3] | Andreas Keil[4] | Matthias J. Wieser[2]

[1]Department of Psychology (Biological Psychology, Clinical Psychology, and Psychotherapy), University of Würzburg, Würzburg, Germany

[2]Department of Psychology, Education, and Child Studies, Erasmus University Rotterdam, Rotterdam, Netherlands

[3]Center for Mental Health, Medical Faculty, University of Würzburg, Würzburg, Germany

[4]Center for the Study of Emotion and Attention, University of Florida, Gainesville, Florida, USA

Correspondence
Yannik Stegmann, Department of Psychology (Biological Psychology, Clinical Psychology, and Psychotherapy), University of Würzburg, Marcusstraße 9-11, Würzburg 97070, Germany.
Email: yannik.stegmann@uni-wuerzburg.de

Abstract

Anxiety is characterized by anxious anticipation and heightened vigilance to uncertain threat. However, if threat is not reliably indicated by a specific cue, the context in which threat was previously experienced becomes its best predictor, leading to anxiety. A suitable means to induce anxiety experimentally is context conditioning: In one context (CTX+), an unpredictable aversive stimulus (US) is repeatedly presented, in contrast to a second context (CTX−), in which no US is ever presented. In this EEG study, we investigated attentional mechanisms during acquisition and extinction learning in 38 participants, who underwent a context conditioning protocol. Flickering video stimuli (32 s clips depicting virtual offices representing CTX+/−) were used to evoke steady-state visual evoked potentials (ssVEPs) as an index of visuocortical engagement with the contexts. Analyses of the electrocortical responses suggest a successful induction of the ssVEP signal by video presentation in flicker mode. Furthermore, we found clear indices of context conditioning and extinction learning on a subjective level, while cortical processing of the CTX+ was unexpectedly reduced during video presentation. The differences between CTX+ and CTX− diminished during extinction learning. Together, these results indicate that the dynamic sensory input of the video presentation leads to disruptions in the ssVEP signal, which is greater for motivationally significant, threatening contexts.

KEYWORDS
anxiety, EEG, oscillation, threat, time frequency analyses, visual processes

1 | INTRODUCTION

Detecting threat in ever-changing environments is crucial for adaptive behavior in animals, including humans. Accordingly, when exploring novel or changing environments, behavioral dispositions are often characterized by heightened vigilance to threat cues, in order to facilitate rapid detection of potentially dangerous situations (Lang et al., 2000; Öhman et al., 2001; Richards et al., 2014). An exaggeration of these mechanisms is a core symptom of anxiety disorders and has been incorporated into the DSM-5, where it is referred to as hypervigilance (American Psychiatric Association, 2013). However, the neurophysiological mechanisms underlying hypervigilance during

anxiety still need to be elucidated. Over the past decade, context conditioning has been established as a laboratory model for learned anxiety (Andreatta & Pauli, 2021; Davis et al., 2010; Maren et al., 2013). During context conditioning, aversive events are administered unpredictably in one of two contexts (threat context), while the other context remains unpaired (neutral context). In contrast to cued fear conditioning, context conditioning involves no threat-predicting signals, making the context the next best predictor for the occurrence of aversive events. Thus the absence of discrete threat-signaling stimuli is thought to result in a sustained state of anxious apprehension (Grillon et al., 2004).

In rodent studies, the immediate surroundings—usually the test cages—serve as context stimuli (Haaker et al., 2019). To translate findings from animal to human research, different physical test rooms have been used to establish distinct contexts in human fear conditioning studies (Klinke et al., 2020; LaBar & Phelps, 2005). However, it is not always feasible nor possible to implement context stimuli through physical rooms. Therefore, basic research has frequently relied on less naturalistic, but more controllable stimuli, like different background colors (Lang et al., 2009; Vansteenwegen et al., 2008), geometrical symbols (Stegmann et al., 2019; Wieser et al., 2016), or colored picture frames (Bublatzky et al., 2014), which are presented on monitor screens. In addition, using simple visual stimuli as contexts enables precise timing of the on- and offsets and facilitates comparability between different contexts. On the other hand, those stimuli often lack ecological validity, as in real life, contexts are encoded as conjunctive representations of multiple elements (Genheimer et al., 2020; Stout et al., 2018, 2019) and organisms are typically able to freely explore the space (Glotzbach et al., 2012).

To overcome these issues, Virtual Reality (VR) provides an optimal tool to create enriched, naturalistic environments and, at the same time, enabling high control over the timing and comparability of context stimuli (Andreatta & Pauli, 2021). For example, Andreatta et al. (2020) used virtual reality to create two different virtual offices that were similar regarding floor plan, size, and complexity, but differed in the arrangement of the furniture. Individuals are also able to freely navigate through the contexts in virtual reality (Glotzbach et al., 2012). Yet, participants remain stationary in order to record psychophysiological parameters (Glotzbach-Schoon, Andreatta, et al., 2013). Consequently, VR is well suited to investigate context conditioning in highly controlled laboratory settings.

A recent fMRI-study used these virtual environments to investigate measures of neural activity during contextual anxiety (Andreatta et al., 2015). Participants were passively guided through the virtual offices on pre-recorded paths, while they received electrical stimulation in one, but never in the other office. Besides successful conditioning, results revealed different neural activity immediately upon the onset of the anxiety-inducing context, compared to later intervals. Increased initial responses to the anxiety-inducing compared to the safe context were found in the primary motor cortex and frontal brain regions, including orbitofrontal (OFC), dorsolateral (dlPFC) and dorsomedial (dmPFC) prefrontal cortex, consistent with the notion that context conditioning prompts conscious awareness of threat contingencies and explicit threat appraisal. Sustained responses were identified in the amygdala and hippocampus, indicating enhanced involvement of the fear/anxiety-network (centered around the amygdala) and neural representations of the spatial map of the context rooms (hippocampus). These results demonstrate that context conditioning is characterized by dynamic involvement of multiple response systems over time.

Given the important role of attention during potentially threatening situations, recent studies have begun to uncover the electrocortical correlates of hypervigilance. To this end, Kastner et al. (2015) investigated steady-state visual evoked potentials (ssVEPs) as direct neurophysiological marker of visual attention during context conditioning. The ssVEP is a oscillatory, electrocortical response to stimuli that are periodically modulated in terms of luminance or contrast (Norcia et al., 2015). Since the frequency of the driving stimulus is known, the ssVEP signal can be reliably separated from the background EEG activity. Importantly, the neural responses are sustained as long as the driving stimulus is presented, making ssVEPs an optimal tool for studying sustained sensory processing during context conditioning, where trials usually last longer than 20 s. Kastner et al. (2015) used pictures of the above-mentioned virtual offices to implement different contexts. The pictures were presented in flickering mode to induce ssVEPs. Results revealed heightened ssVEP amplitudes throughout the whole 20 s presentation of the aversive conditioned compared to the neutral context, suggesting cortical facilitation of perceptual processing during the threatening context as a visuocortical correlate of hypervigilance. These results were conceptually replicated using a combined cue and context conditioning task (Kastner-Dorn et al., 2018) and parallel results of enhanced ssVEP amplitudes during contextual threat using geometrical symbols as visual stimuli (Stegmann et al., 2019; Wieser et al., 2016). Taken together, these finding are in line with a substantial body of research demonstrating heightened electrocortical activity in response to threat-associated stimuli (Miskovic & Keil, 2012).

In naturalistic settings, however, visual input is not static as dynamic environments as well as body-, head- and gaze-movements lead to constant changes in the stream

of visual information. This is especially relevant for potentially threatening environments, in which changes in sensory input (e.g., the sudden occurrence of a predator), rather than the static environment per se, signal upcoming danger. Therefore, the next crucial step is to quantify visuocortical responding to more ecologically valid contextual stimuli. To this end, the present study utilized video stimuli of virtual offices to implement differential context conditioning. Similar to Andreatta et al. (2015), participants were passively guided through the offices in order to establish spatial representations of the contexts. The two main goals of this study were to (1) successfully induce ssVEPs using video stimuli and to (2) investigate changes in visuocortical responding during potentially threatening contexts induced by differential context conditioning. Here, we tested the hypothesis if aversive context conditioning prompts enhanced visuocortical responses to threatening compared to safe contexts, as measured by ssVEPs.

2 | METHOD

2.1 | Sample

In total, 40 participants participated in the experiment, of which two were excluded due to data recording failures during the experiment. The final sample included 38 participants (24 females, mean age ± SD: 23.63 ± 3.72 years). Participants were required to be between 18 and 35 years old, free of any family history of photic epilepsy, free of any mental health or neurological disorders (self-report), and to have normal or corrected vision. All participants gave written informed consent and were paid 15 € or received course credits. All procedures were approved by the ethics committee of the University of Würzburg but have not been preregistered.

2.2 | Stimuli and apparatus

Videos pre-recorded from virtual reality served as context stimuli. The virtual environment was created with Valve Corporation's Source Engine (Bellevue, USA) and has been successfully used in other context conditioning studies (Andreatta et al., 2020). During each video, the participant started in a corridor in front of one of two different office rooms. After the door opened, the participant was passively guided through the office on a pre-recorded pathway. After about 35 s, the participant left the office room and the video ended. There was one pathway in the clockwise and one in the counterclockwise direction per room. The two virtual offices were designed to be similar regarding size, floor and lighting and only differed in furniture arrangement, window style and decoration (see Figure 1). Video stimuli were counter-balanced for conditions (CTX+ vs. CTX−) across participants. All stimuli were presented on a 19-inch monitor (resolution = 1024×768 pixels) with a vertical refresh rate of 60 Hz, located ca. 100 cm in front of the participant, using the Presentation software (Neurobehavioral Systems, Inc., Albany, CA, USA). The videos spanned a visual angle of 14.75° horizontally and 11.14° vertically. In order to evoke ssVEPs, video stimuli were presented continuously while an overlaying black frame was presented in flickering mode in 20 Hz. Before conducting the experiment, we ensured that there were no delays in video display due to technical constraints (e.g., monitor responsiveness).

Aversive unconditioned stimuli (US) were 20 ms electric pulse trains (2 ms pulse width, 25 Hz), which were
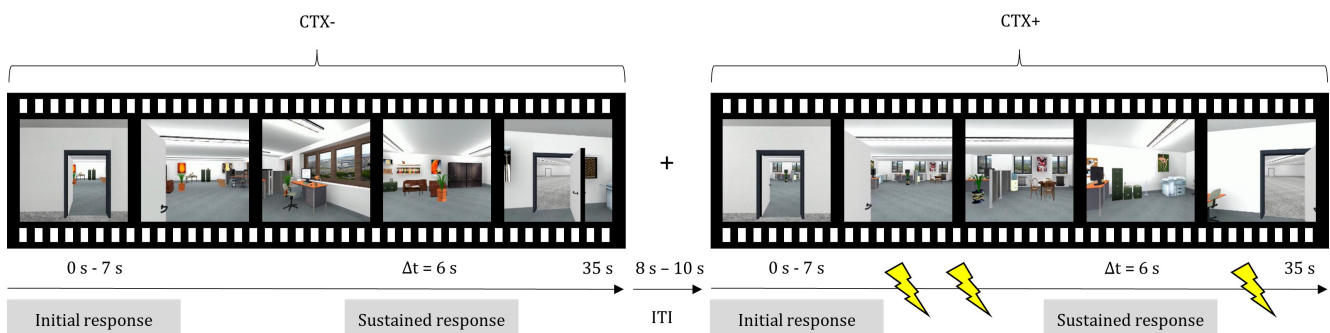
FIGURE 1 Experimental design. Participants watched videos, in which they were guided through one of two different virtual offices. In one office (threat context; CTX+), 0 to 3 US were presented unpredictably. No US were presented in the other office (safety context; CTX−). Videos were presented in 20 Hz flicker frequency to evoked ssVEPs. To analyze ssVEPs and skin conductance responses during the initial response window, no US was presented during the first 7 s after video onset. At a random timepoint during the second half of each video, US-delivery was omitted for an interval of 6 s to analyze sustained ssVEP responses.

delivered to the left calf through surface bar electrodes consisting of two gold-plated stainless-steel disks of 9 mm diameter and 30 mm spacing. The electric stimuli were generated by a constant current stimulator (Digitimer DS7A, Digitmer Ltd., Welwyn Garden City, UK). Prior to the actual experiment, the US intensity was adjusted to the individual pain-threshold. Thus, participants received two series of increasing and decreasing intensities until they reached a level they described as "just noticeable pain"—corresponding to 4 on a scale from 0 (no pain at all) to 10 (unbearable pain). The individual US intensity was determined by calculating the mean of the four series' final intensities and then adding 30% to avoid habituation. The resulting intensities and subjective pain ratings were 1.89 ± 1.02 mA (mean intensity $\pm$ SD) and 5.32 ± 1.04 (mean pain rating $\pm$ SD).

2.3 | Procedure

Participants were seated in a sound-attenuated, dimly lit testing room, where EDA-electrodes and the EEG-net were applied. The study consisted of a pre-acquisition, acquisition and extinction phase. During pre-acquisition each video was presented once (2 videos per room), and no US was delivered (see Figure 1). The ITI had a random duration between 8 and 10 s. Pre-acquisition was followed by two rating trials, which started as normal trials, but were paused after about 10 s, in which a visual analog scale was presented to collect online ratings. During this procedure, participants were asked to rate the current room regarding valence, arousal (both 9-point Likert-scales; from 1 = very unpleasant/ very calm to 9 = very pleasant/ very exciting), anxiety and US-expectancy (both visual analogue scales from 0 = not anxious/ not likely to 100 = very anxious/ very likely). As soon as the participant finished the rating procedure, the video continued. Rating trials were excluded from physiological and electrocortical analysis. Acquisition consisted of 16 video trials (8x CTX+ and 8x CTX−) plus four additional rating trials after the first half and in the end of the phase. US-delivery in the CTX+ started after 7 s and was omitted after 32 s to ensure that participants received US only inside of the office room. Per CTX+, zero to three US were unpredictably delivered with an interval of at least 5 s between two US. US were also presented during CTX+ rating trials, resulting in a total of 15 US presentations. Importantly, a time interval of 6 s was randomly chosen during the last half of each trial, in which no US was delivered. To enable averaging across trials, the random intervals started at integer seconds, thus comprising ssVEP starting with the same phase, given 20 Hz stimulation. This interval

was later used for EEG-analysis without confounding US-presentations. The extinction phase was identical to acquisition regarding trials and timing, but no US were delivered. Participants were instructed to reduce eye-movements and focus on a fixation cross that was centrally presented throughout the experiment.

2.4 | Physiological data processing

Skin conductance was recorded using two silver-silver chloride electrodes filled with 0.5% NaCl electrode gel and placed on the thenar and hypothenar eminences of the participants' non-dominant palmar surface. The signal was recorded with a V-Amp amplifier and Brain Vision Recorder Software (BrainProducts Inc., Munich, Germany). A sampling rate of 1000 Hz and a notchfilter at 50 Hz were applied. Analysis was then performed using Brain Vision Analyzer Software (BrainProducts Inc., Munich, Germany). For each experimental condition, the trough-to-peak values within 1 s to 6 s after video-stimulus onset was scored manually, square-root-transformed and then divided by the participant's maximum SCR to a context onset. SCRs smaller than 0.02 μS were scored as zero responses before transformation (Boucsein et al., 2012).

2.5 | EEG recording and data processing

EEG data analysis was conducted and is reported according to published guide lines (Keil et al., 2014). Electrocortical brain activity was recorded using a 129 electrodes Electrical Geodesics System (EGI, Eugene, OR) referenced to the vertex electrode (Cz), with a sampling rate of 250 Hz and an online band-pass filter of 0.1–100 Hz. Electrode impedances were kept below 50 kΩ. Subsequent data processing occurred offline using the EMEGS software for Matlab (Peyk et al., 2011). In a first step, all data were filtered using a 40-Hz low-pass filter (cut-off at 3 dB point; 45 dB/octave, 19th order Butterworth), before extracting epochs from 600 ms pre- to 6900 ms post-onset for the initial response and from 400 ms to 5900 ms during the late interval (a randomly jittered 6000 ms interval between 18,000 ms and 27,000 ms post-onset) for the sustained electrocortical processing. Following the guidelines for the statistical correction of artifacts in dense array studies procedure (Junghofer et al., 2000), we first detected individual channel artifacts based on the original recording reference (Cz), before data were re-recorded to the average reference to identify global artifacts. Bad sensors within individual trials were identified based on rejection criteria for the distributions of the maximum absolute amplitude, standard deviation, and gradient. Contaminated

trials were removed if they included more than 20 bad sensors. After rejection, contaminated sensors of the remaining epochs were interpolated using weighted spherical splines fit to all remaining sensors. The retention rate for initial and sustained responses were $64.5 \pm 23.5\%$ and $78.7 \pm 20.0\%$ (M ± SD), respectively. Remaining epochs were averaged separately for the two context conditions and the three main phases of the experiment. To reduce the impact of volume conductance, the current source densities (CSD) of the time-averaged data were calculated. The CSD transformed data were then submitted to a Fast-Fourier-algorithm on a time interval between 2000 and 6500 ms post-onset for the initial response and from 1400 ms to 5900 ms during the sustained response interval (a randomly jittered 6000 ms interval between 18,000 ms and 27,000 ms post-onset). The first 2000 ms after stimulus onset were omitted since the virtual door to the office opens between 1000 and 2000 ms after stimulus onset. The time window of the sustained response interval was chosen to be the same in total length as the initial response interval to facilitate comparability between initial and sustained responses.

In a next step, we obtained the signal-to-noise ratio (SNR) for the driving frequency by dividing the power of the 20 Hz frequency by the mean of the spectral power at six adjacent frequency bins, leaving out the two immediate neighbors. The SNR is a unitless measure which accounts for both the evoked signal and the random noise in the data and has recently been used in other ssVEP paradigms as well (Barry-Anwar et al., 2018; Stegmann et al., 2020). The CSD-transformed ssVEP signals for a representative electrode (Oz), the Fast-Fourier-Transformation on these ssVEPs, the time-frequency representations of the driving frequencies, and the topography of their SNRs averaged across all subjects and conditions are shown in Figure 2. For statistical analysis, the ssVEP activity was pooled across the Oz and 7 surrounding electrodes (EGI sensors 70, 71, 72, 74, 75, 76, 82, 83).

2.6 | Statistical analyses

The mean SCR to context onset and the mean ssVEP amplitudes during the initial and sustained response
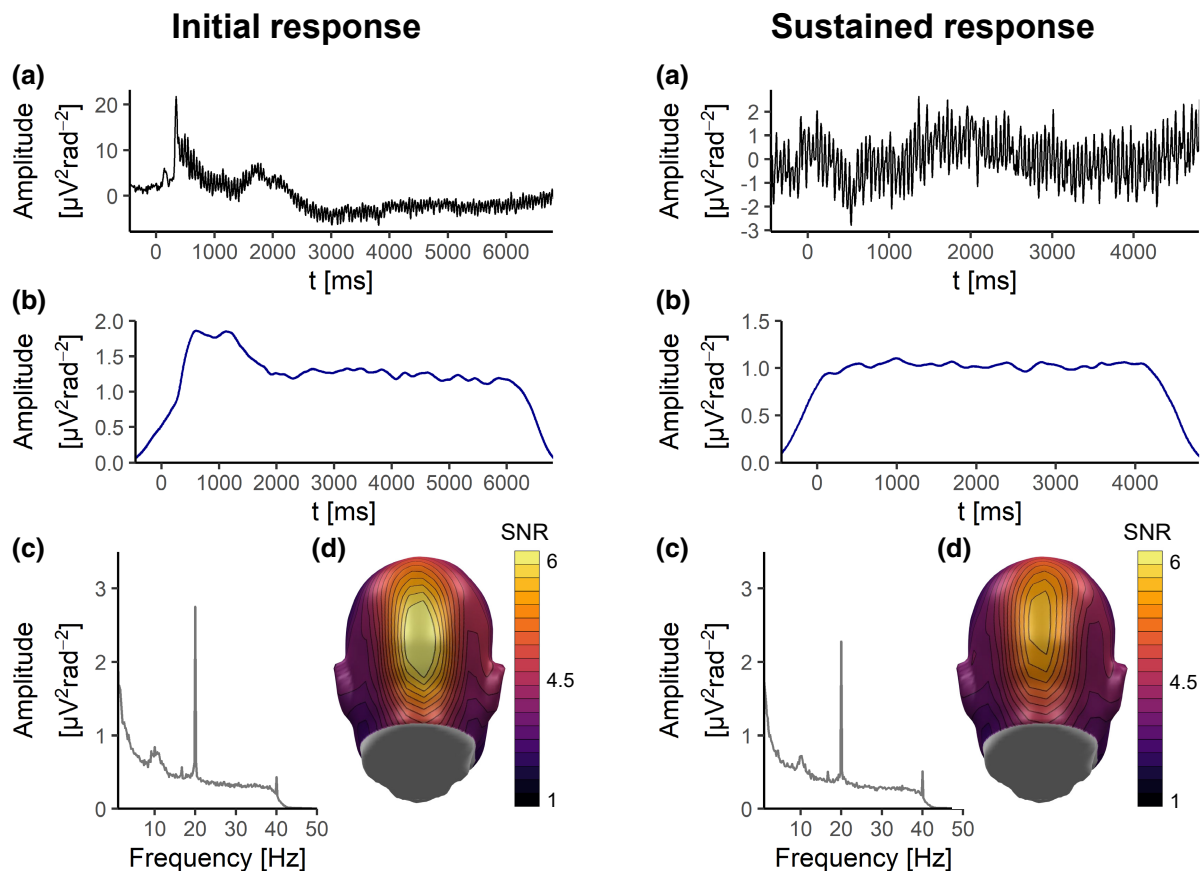
FIGURE 2 Characteristics of the grand averaged ssVEP signal during the initial and sustained response window across all participants and conditions at Oz (sensor 75): (a) time-domain representation of the CSD-transformed ssVEP response. (b) Time-frequency analysis of the Hilbert-transformed 20 Hz driving frequency. (c) Frequency-domain representation. (d) Topographies of the signal-to-noise ratio.

PSYCHOPHYSIOLOGY SPR

window were analyzed separately with mixed-measure analysis of variances (ANOVA) with the within-subject factors context (CTX+ vs CTX−) and phase (Acquisition vs Extinction). The same procedure was carried out for valence, arousal, anxiety, and US-expectancy ratings. Differences in the pre-acquisition phase of the experiment were analyzed with simple t-tests. Significant effects were followed up using ANOVAs and t-tests where appropriate. A significance level of 0.05 was used for all analyses. Throughout this manuscript, the partial η^2 (η_p^2) or Cohen's d (d) and their 95% confidence interval are reported as standardized effect sizes.

3 | RESULTS

3.1 | Pre-Acquisition phase

During pre-acquisition, CTX+ and CTX− did not differ regarding valence, $t(37) = -0.42$, $p = .675$, $d = -0.07$ [CI: −0.39; 0.25], anxiety, $t(37) = -1.56$, $p = .127$, $d = -0.25$ [CI: −0.57; 0.07], skin conductance responses, $t(33) = 0.22$, $p = .826$, $d = 0.04$ [CI: −0.30; 0.37], and ssVEP amplitudes during the initial, $t(31) = 0.25$, $p = .806$, $d = 0.04$ [CI: −0.30; 0.39], or the sustained response window, $t(37) = 1.70$, $p = .098$, $d = 0.28$ [CI: −0.05; 0.60]

(see Figure 3). Surprisingly, there was a significant difference between CTX+ and CTX− for arousal ratings, $t(37) = -2.19$, $p = .035$, $d = -0.35$ [CI: −0.68; −0.02], indicating higher arousal ratings for CTX+ compared to CTX−, although no US had been delivered yet. However, this difference is only present for arousal ratings and video stimuli were counterbalanced across participants, so this finding is most likely a false positive.

3.2 | Acquisition and extinction phase

3.2.1 | Steady-state visual evoked potentials

Regarding the initial response window, there was neither a significant main effect of context, $F(1,37) = 0.03$, $p = .857$, $\eta_p^2 < .01$ [CI: 0.00; 0.05], phase, $F(1,37) = 2.87$, $p = .099$, $\eta_p^2 = .07$ [CI: 0.00; 0.22], nor a Context × Phase interaction, $F(1,37) = 0.18$, $p = .674$, $\eta_p^2 < .01$ [CI: 0.00; 0.09] (see Figure 4).
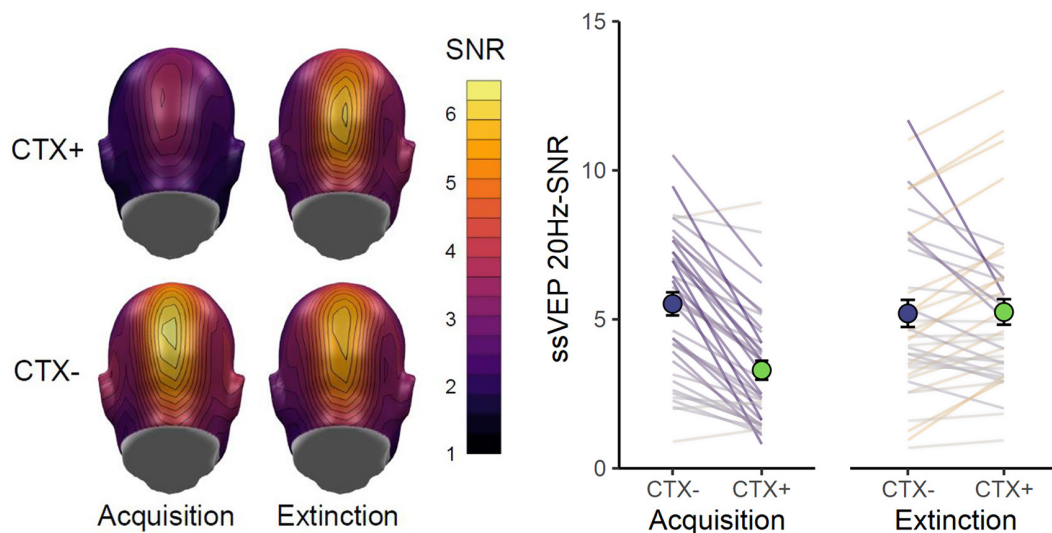
During the sustained response window, there was a significant main effect of context, $F(1,37) = 30.64$, $p < .001$, $\eta_p^2 = .45$ [CI: 0.24; 0.59], and phase, $F(1,37) = 18.42$, $p < .001$, $\eta_p^2 = .33$ [CI: 0.13; 0.49], which were further qualified by a significant Context × Phase interaction, $F(1,37) = 41.73$, $p < .001$, $\eta_p^2 = .53$ [CI: 0.33; 0.65]. Post-hoc t-tests indicated
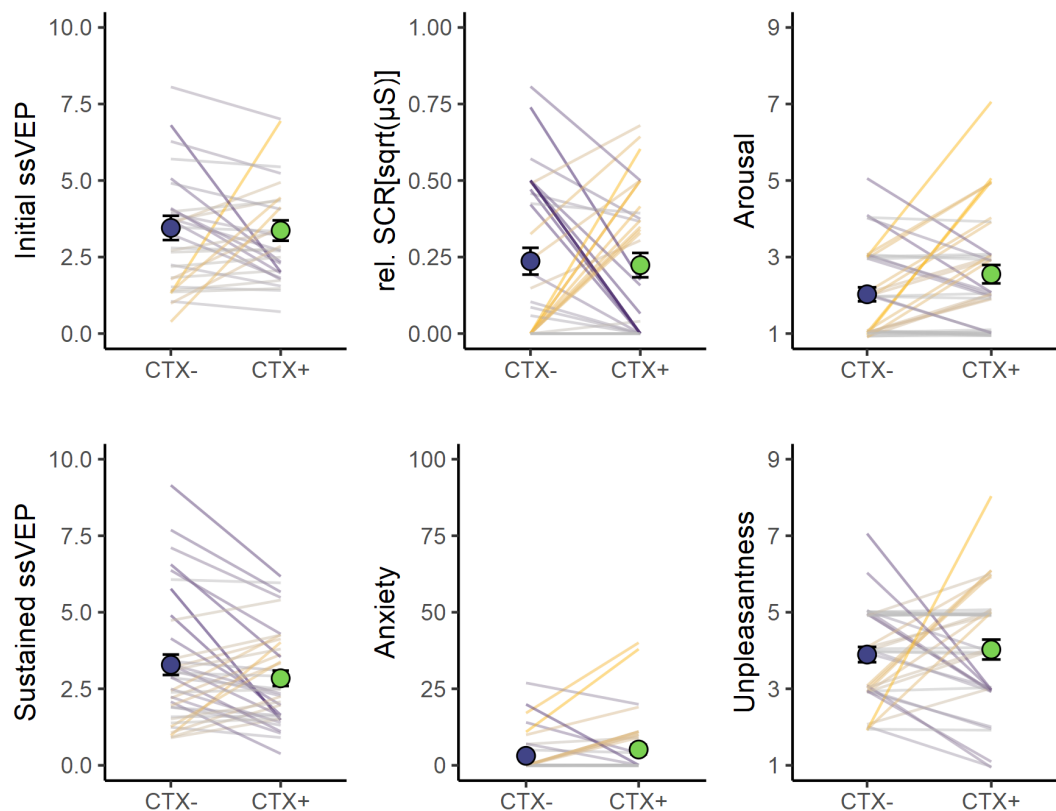
FIGURE 3 Mean defensive responses (±SEM) during the pre-acquisition phase. Orange lines denote increasing and purple lines denote decreasing responses from CTX− to CTX+.
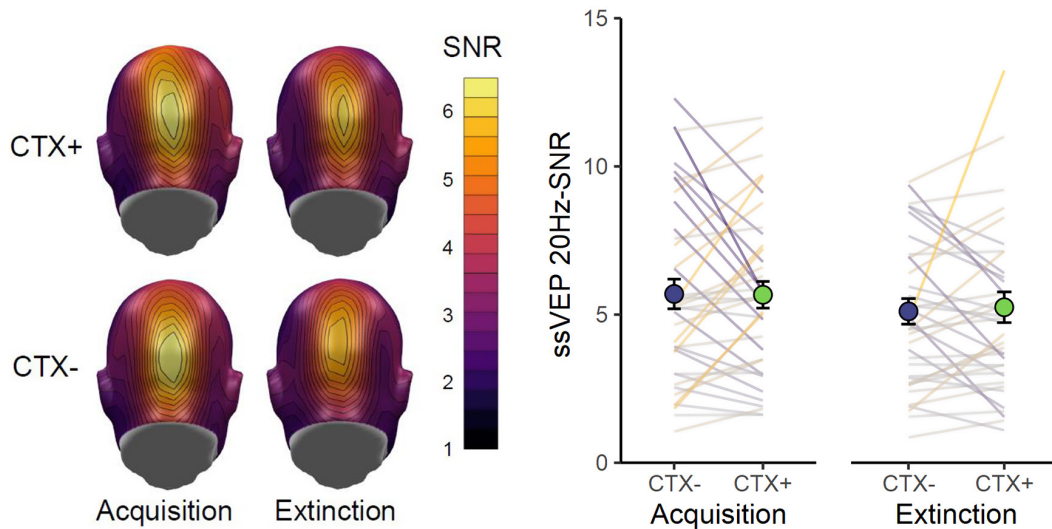
FIGURE 4 Topographies (left) and the corresponding mean (±SEM) ssVEP SNRs (right) to the context cues during the initial response window. Orange lines denote increasing and purple lines denote decreasing responses from CTX− to CTX+.


FIGURE 5 Topographies (left) and the corresponding mean (±SEM) ssVEP SNRs (right) to the contexts during the sustained response window. Orange lines denote increasing and purple lines denote decreasing responses from CTX− to CTX+.

stronger ssVEP SNRs to the CTX− compared to the CTX+, $t(37) = 9.06$, $p < .001$, $d = 1.47$ [CI: 1.00; 1.93], during acquisition but not during extinction, $t(37) = −0.18$, $p = .862$, $d = −0.03$ [CI: −0.35; 0.29] (see Figure 5).

3.2.2 | Exploratory analyses

First, an alternate explanation was examined that the increased ssVEP amplitude to the CTX− compared to the CTX+ was due to electrical stimuli that were presented during CTX+ only, prior to the sustained response interval. To that end, the ssVEP data was reanalyzed excluding

any trials in which electrical stimuli were presented within 5000 ms before the sustained response interval. Consequently, 2.94 ± 1.41 (mean ± SD; range = [0.5]) trials per participant were removed from the analysis. However, the differences between CTX+ and CTX− in the remaining trials remained significant, $t(37) = 7.20$, $p < .001$, $d = 1.17$ [CI: 0.75; 1.58], suggesting that the electrical stimulation did not decrease the ssVEP SNR to the CTX+. For a more detailed exploratory analysis, CTX+ trials were subdivided into four categories according to the total number of US (0–3) presented prior to the sustained response interval (see Figure 6a). Interestingly, ssVEP amplitudes were marginally significantly higher for the CTX+ trials without US
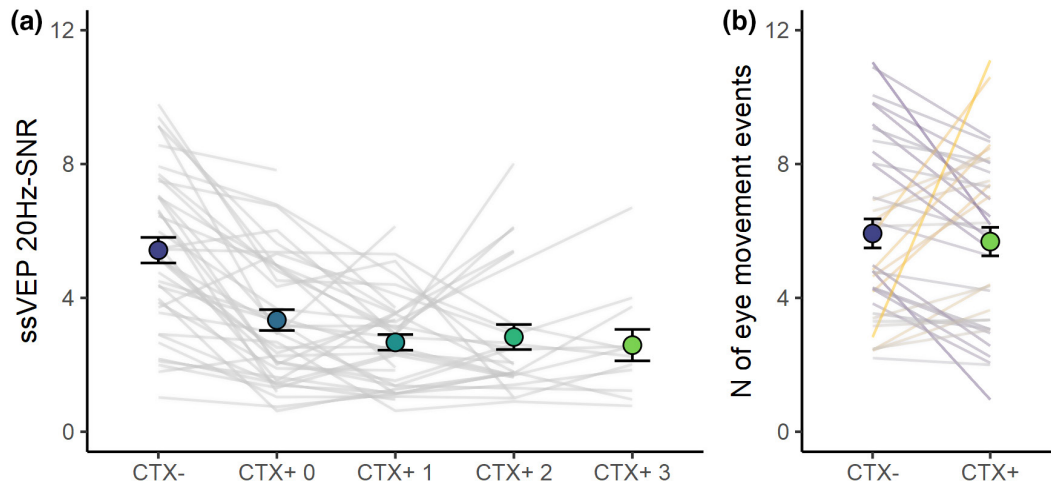
FIGURE 6 Exploratory analyses of the ssVEP and EOG signal during the sustained response window. (a) Mean ssVEP SNR (±SEM) during the CTX− and CTX+ as a function of the total number of preceding US, ranging from 0 (CTX+ 0) to 3 (CTX+ 3). Please note the unequal sample sizes per condition due to randomization of US timing. (b) Mean number of eye-movement events (±SEM) as indexed by substantial EOG signal changes during the CTX+ and CTX−. Orange lines denote increasing and purple lines denote decreasing responses from CTX− to CTX+.

compared to the CTX+ trials with one US prior to the response window, $t(33) = 1.95$, $p = .059$, $d = 0.33$ [CI: −0.01; 0.68], while there were no differences among the reminder of the CTX+ trials, all $ps > .259$. Critically, all CTX+ trials, especially CTX+ trials without preceding US presentations elicited significantly smaller ssVEP amplitudes than CTX− trials [0 US: $t(36) = 7.11$, $p < .001$, $d = 1.17$ [CI: 0.74; 1.58]; 1 US: $t(34) = 9.34$, $p < .001$, $d = 1.58$ [CI: 1.07; 2.07]; 2 US: $t(24) = 5.75$, $p < .001$, $d = 1.15$ [CI: 0.63; 1.65]; 3 US: $t(11) = 3.08$, $p = .011$, $d = 0.89$ [CI: 0.20; 1.55]].

Another explanation for the decreased ssVEP SNR to the CTX+ is that there was heightened oculomotor activity during the threat context, which might have led to a disruption of the ssVEP signal. To quantify eye movement, we calculated the Euclidean norm of the signals recorded by the EOG electrodes measuring horizontal and vertical eye-movements at the level of single trials. Specifically, the bipolar difference between pairs of EOG electrodes entered this analysis and horizontal and vertical signals were combined as the square root of the sum of squares of horizontal and vertical EOG, to approximate a global measure of oculomotor activity. Eye movement events were defined as sample points where the difference of the normed EOG signal and the subject mean exceeded three standard deviations. The minimum interval between two eye-movement events was set to 50 ms. Comparing the mean number of eye movement events between CTX+ and CTX− (see Figure 6b) yielded no significant differences, $t(36) = 0.59$, $p = .560$, $d = 0.10$ [CI: −0.23; 0.42]. Eye movement as indexed by the EOG signal did not differ between conditions, and consequently, might not have had an impact on the ssVEP signal.
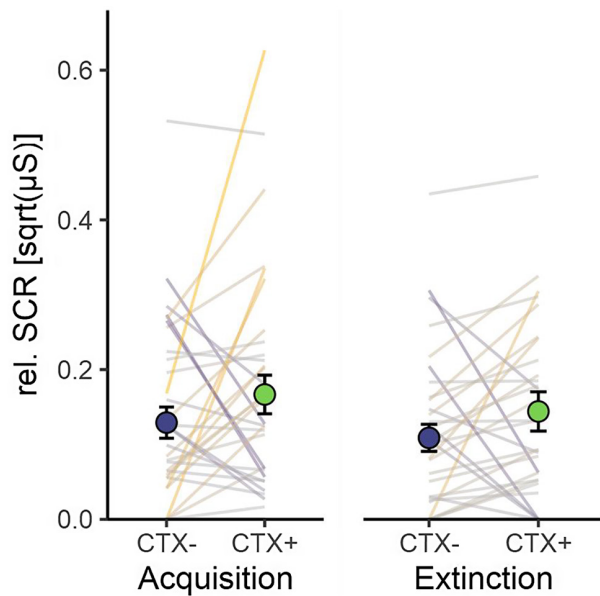
3.2.3 | Skin conductance responses

Four participants were removed from SCR analysis because they showed no quantifiable skin conductance response. The ANOVA for the remaining participants showed no significant main effect of phase, $F(1,33) = 1.29$, $p = .263$, $\eta_p^2 = .04$ [CI: 0.00; 0.18], or phase × context interaction, $F(1,33) = 0.01$, $p = .939$, $\eta_p^2 < .01$ [CI: 0.00; 0.01]. The main effect of context, $F(1,33) = 3.78$, $p = .060$, $\eta_p^2 = .10$ [CI: 0.00; 0.27] was marginally significant, suggestive of slightly higher skin conductance responses to the onset of the threat context compared to the neutral context (Figure 7).

3.2.4 | Ratings

Phase × Context ANOVAs revealed significant main effects of phase (all $ps < .001$) and context (all $ps < .001$), which were further qualified by phase × context interactions for valence, $F(1,37) = 19.27$, $p < .001$, $\eta_p^2 = .34$ [CI: 0.14; 0.50], arousal, $F(1,37) = 28.04$, $p < .001$, $\eta_p^2 = .43$ [CI: 0.22; 0.57], anxiety, $F(1,37) = 10.57$, $p = .002$, $\eta_p^2 = .22$ [CI: 0.05; 0.39], and US-expectancy ratings, $F(1,37) = 41.93$, $p < .001$, $\eta_p^2 = .53$ [CI: 0.33; 0.65]. During acquisition, participants rated the CTX+ as more unpleasant, with higher emotional arousal, more anxiogenic, and more associated with an US, than the CTX− (see Figure 8 and Table 1 for statistics of the post-hoc t-tests). During extinction, ratings to the CTX+ decreased, while ratings to the CTX− did not change. At the end of extinction, however, there were still significant differences between CTX+ and CTX−.

FIGURE 7 Mean skin conductance responses (±SEM) to video stimulus onsets. Orange lines denote increasing and purple lines denote decreasing responses from CTX− to CTX+.

4 | DISCUSSION

In the present study, a differential context conditioning paradigm was used to investigate visuocortical activity during potentially threatening, naturalistic scenes. For the first time, steady-state visual evoked potentials were induced by presentations of flickering video stimuli. During each video, participants were passively guided on a pre-recorded pathway through one of two virtual offices. To capture physiological and behavioral responding during potential threat, skin conductance responses were collected next to verbal reports of subjective valence, arousal, anxiety, and US-expectancy.

Results demonstrated successful context conditioning for subjective measures of defensive responding. After acquisition, the threat context elicited higher arousal, unpleasantness, anxiety, and US-expectancy ratings than the neutral context. These results were substantiated by a marginally significant effect of context conditioning on skin conductance responses to the onset of the video stimuli. Consequently, these findings contribute to a large body of literature, demonstrating enhanced defensive responses during situations of potential threat (Andreatta et al., 2015; Glotzbach-Schoon, Tadda, et al., 2013; Grillon et al., 2004, 2006).

To quantify sustained visual activity, steady-state visual evoked potentials were measured during an initial as well as a sustained time window. The initial time window comprised the first 7 s after stimulus onset, from which the first 2 s were omitted from statistical analysis, because participants were not aware of the condition at

this timepoint due to closed doors. The sustained time window was a randomly chosen interval of 5 s during the second half of the video stimulus presentation, which was not further signaled to the participant. The steady-state responses evoked by the flickering video stimuli revealed generally high signal-to-noise ratios and descriptive topographical analysis showed broad visuocortical activity over the occipital scalp (see also Figure 2), paralleling findings of other contextual threat ssVEP studies (Kastner et al., 2015; Kastner-Dorn et al., 2018; Wieser et al., 2016; Wieser & Keil, 2014). These results suggest successful induction of robust ssVEP signals by flickering video stimuli, highlighting the potential usefulness of this measure over for example skin conductance, where several non-responders had to be excluded from the present study. Analyzing the signal-to-noise ratios of the 20 Hz driving frequency during the initial response window, however, revealed no differences between the threatening and the neutral context for acquisition or extinction learning.

These findings are in contrast to Kastner et al. (2015), who found differential effects of context conditioning throughout the whole duration (20 s) of the stimulus presentation, using flickering screenshots of the virtual offices. However, fine-grained temporal analyses revealed that these effects were mainly driven by differences throughout the later time intervals of the context presentation (beginning from 8 s after context onset), suggesting that changes in visuocortical activity due to potential threat do not appear immediately but become operational throughout longer periods of potential threat, especially with contexts being more complex. Likewise, in the present study, effects of context conditioning on ssVEP amplitudes might not have occurred during the initial response window. One possible explanation could be that participants may have learned that the first few seconds after context onset were relatively safe because no US was presented during the initial response windows. Thus, participants may have felt less aroused at the beginning of a trial, which could also be reflected in the relatively small differential SCRs to threat and safety contexts. On the other hand, it is not surprising that potential threat is associated with effects on a larger timescale, as danger is not yet imminent and there is no need for a rapid engagement of defensive mechanisms (Fanselow, 1994). This idea is supported by the results of the fMRI study by Andreatta et al. (2015), demonstrating that during sustained context presentations different neural regions are activated than during the initial response window. Crucially, enhanced amygdala activity was only found during the sustained response window. Given its important role in driving changes in cortical sensory processing (Miskovic & Keil, 2012), the absence of amygdala activity could be accompanied by a
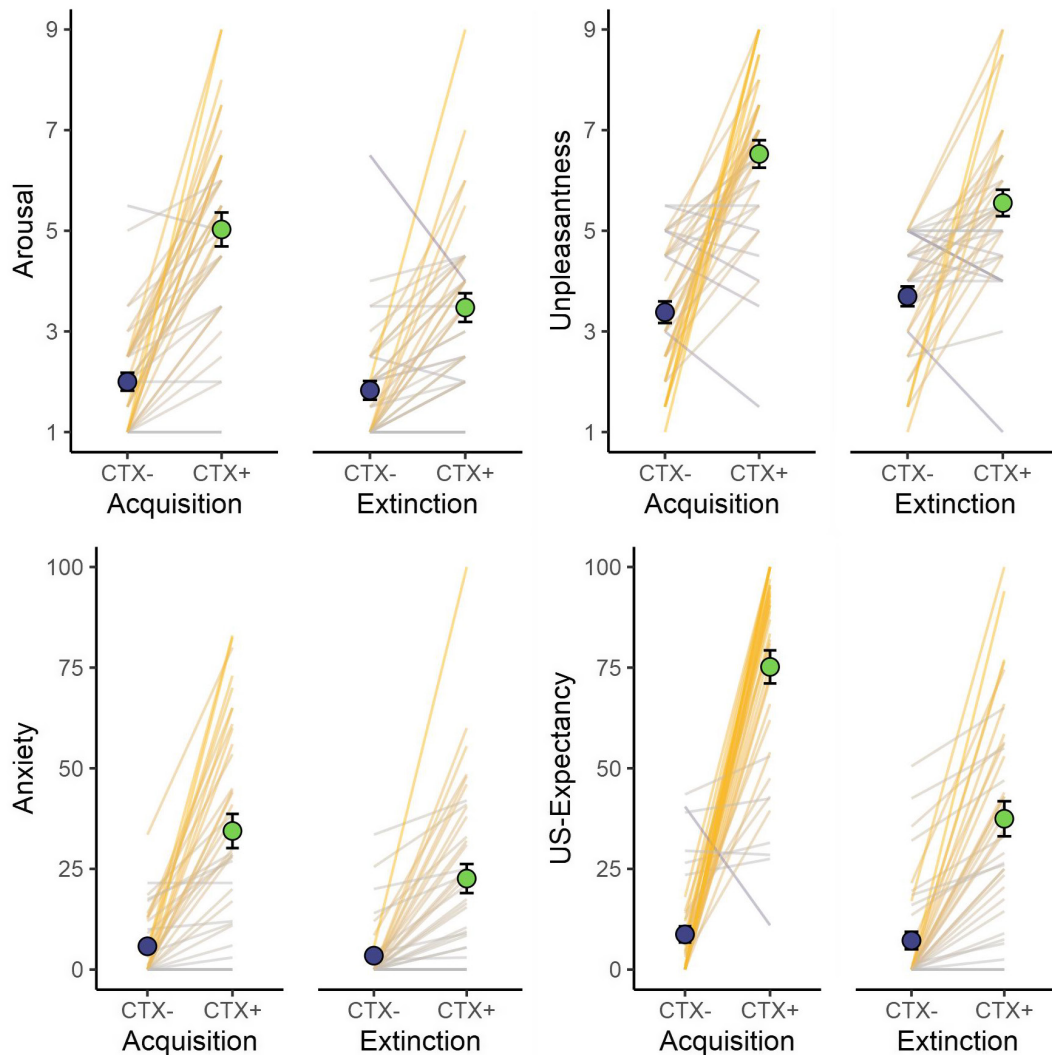
FIGURE 8 Mean arousal, unpleasantness, anxiety and US-expectancy ratings (±SEM) of the video stimuli. Orange lines denote increasing and purple lines denote decreasing responses from CTX− to CTX+.

lack of differential visuocortical responding during the initial presentation of the contexts.

During the sustained response window, the present study observed differences in ssVEP amplitudes between the threatening and neutral context. Visuocortical activity during the threatening context was decreased compared to the neutral context. This is in line with the notion that free viewing of moving, complex, and motivationally relevant video prompts variable top-down modulation into visual cortex that may interfere with the regularity (phase) of the ssVEP signal, resulting in paradoxical reduction of the visuocortical signal for the more relevant of two stimuli. This result sheds new light on the neural account of visuocortical responding to video stimuli, and also prompts questions for future research: Is this robust interference effect an epiphenomenon of the ssVEP technique, or is it a reflection of true reduction in visuocortical engagement? Additional work is needed, ideally combining ssVEPs and

other metrics of visuocortical processing. Recently, several authors have begun to investigate how transient changes in a stimulus train affect the ssVEP response. To this end, Bekhtereva et al. (2018) used a rapid serial visual presentation (RSVP) stream, which included pictures of neutral und unpleasant scenes. To induce ssVEPs, the RSVP stream of changing, rather than constant scenes, was presented in different frequencies ranging from 3 to 8.75 Hz. As expected, transient changes from neutral to unpleasant stimuli were associated with enhanced ssVEP amplitudes for the 3 Hz, 4 Hz, and 8.57 Hz frequency. Using a flicker frequency of 6.66 Hz, however revealed the exact opposite, i.e. changes from neutral to unpleasant stimuli actually decreased ssVEP response amplitudes. This finding is specific for the 6.66 Hz frequency, an effect that has been replicated in independent experiments (Riels et al., 2020). By using simulation analysis, Bekhtereva et al. (2018) demonstrated that this effect is likely due to linear superpositions

TABLE 1 Statistical details of the post-hoc *t*-tests following the phase x context interaction effects for rating data

	Post-hoc *t*-test	*t*	*p*	*d*	CI$_{95\%}$
Unpleasantness	Acq: CTX+ vs CTX−	7.67	.001	1.24	[0.81; 1.66]
	Ext: CTX+ vs CTX−	5.27	.001	0.85	[0.48; 1.22]
	CTX+: Acq vs Ext	5.96	.001	0.97	[0.58; 1.35]
	CTX−: Acq vs Ext	1.86	.071	0.30	[−0.62; 0.03]
Arousal	Acq: CTX+ vs CTX−	8.78	.001	1.42	[0.97; 1.87]
	Ext: CTX+ vs CTX−	5.50	.001	0.89	[0.51; 1.26]
	CTX+: Acq vs Ext	6.39	.001	1.04	[0.64; 1.43]
	CTX−: Acq vs Ext	1.21	.234	0.20	[−0.13; 0.52]
Anxiety	Acq: CTX+ vs CTX−	7.09	.001	1.15	[0.73; 1.56]
	Ext: CTX+ vs CTX−	5.55	.001	0.90	[0.52; 1.27]
	CTX+: Acq vs Ext	4.15	.001	0.67	[0.32; 1.02]
	CTX−: Acq vs Ext	1,83	.075	0.30	[−0.03; 0.62]
US-Expectancy	Acq: CTX+ vs CTX−	11.71	.001	1.90	[1.36; 2.43]
	Ext: CTX+ vs CTX−	7.27	.001	1.18	[0.76; 1.59]
	CTX+: Acq vs Ext	7.99	.001	1.30	[0.86; 1.72]
	CTX−: Acq vs Ext	.63	.532	0.10	[−0.22; 0.42]

Note: *t*-tests df = 37.

Abbreviations: Acq, acquisition; Ext, extinction.

of the ERPs, which are evoked by the individual images of the RSVP, prompting destructive interference and thus ultimately reducing ssVEP amplitudes. If linear superpositions of ERPs resulted in decreased ssVEP amplitudes, similar mechanisms ought to be expected with presentation frequencies of integer multiples of the 6.66 Hz frequency. Crucially, the 20 Hz frequency used in the current study is indeed an integer multiple of 6.66 Hz. Therefore, the reduced visuocortical responses during the threatening context suggest a greater disruption of the ssVEP signal caused by the constant stream of visual input and enhanced ssVEP amplitudes during potential threat could be expected for different presentation frequencies.

Notably, the present findings parallel results of a recent study (Campagnoli et al., 2019), utilizing ssVEPs to investigate visuocortical responses to subtle changes of emotional facial expression. The authors presented flickering pictures of neutral facial expressions, which throughout the trial changed to either another neutral or to an emotional facial expression of the same individual. Paralleling findings in Bekhtereva et al. (2018) and Riels et al. (2020), it was observed that transient changes in facial expression perturbed the ssVEP signal and led to a reduction of the time-varying ssVEP amplitudes lasting about 800–1000 ms. This is also in support of the idea that driven neural oscillation are disrupted by transient brain responses, as underlying circuits receive additional afferent input, interfering with the ssVEP phase and ultimately resulting in a reduction of ssVEP amplitude (Campagnoli et al., 2019; Moratti et al., 2007; Muller et al., 2008). Applied to the

present paradigm, video stimuli can be considered as a continuous stream of afferent input, as each frame of the video stimulus contains additional sensory information. This is an important aspect, since the neural mechanisms underlying perceptual processing of continuously changing visual stimuli are not well understood. While studies using static images to induce ssVEPs usually target specific low-level features of the visual stimulus, like orientation, contrast or color (Keil et al., 2013; McTeague et al., 2015) or employ pictures of static facial expressions to investigate social attentional processing (Stegmann et al., 2020; Wieser & Keil, 2011, 2014), the video stimuli of the present study consist of a complex composition of different low-level features that, in addition, change over time. To improve our understanding of visuocortical processing of video stimuli, future studies may wish to systematically investigate visuocortical responding to visual stimuli that continuously change in one low-level feature, at different driving frequencies, and adding additional imaging modalities such as fMRI.

It is also important to note that we used videos of virtual offices, but not immersive VR. In a recent study, Stolz et al. (2019), measured late positive potentials (LPPs) during conditioning using a combined head-mounted display and EEG setup. Consistent with the findings of Kastner et al. (2015), the authors found increased LPPs to the threat context compared to safety context. However, to record enough trials to achieve a sufficient SNR for the LPP, the authors presented each context for only 2 s. In the current study, we used ssVEPs to quantify continuous

visuocortical activity. Although LPPs and ssVEPs are both measures related to attention allocation and are sensitive to motivational significance, ssVEPs are capable of recording visuocortical activity on a larger time scale, making them more suitable for studying the temporal dynamics of attention allocation.

It is also important to mention that we were able to rule out the alternative explanations that reduced ssVEP signals during the threatening context were the result of artifacts caused by previous electrical stimulation or excessive eye movements. In addition, effects of context conditioning were relatively stable throughout extinction learning for measures of defensive responding, while visuocortical responses did not show differences related to the threat/safe context during extinction. This is in line with results of recent studies analyzing ssVEPs on single-trial level that demonstrated a reduction of threat-enhanced ssVEP amplitudes after as few as two unreinforced CS+ presentations (McTeague et al., 2015; Wieser et al., 2014).

In conclusion, situations of potential threat prompt activation of the defensive system, which is associated with facilitated defensive responses on a subjective and physiological level (Glotzbach et al., 2012; Grillon et al., 2004). Findings regarding ssVEP amplitudes demonstrated generally high signal-to-noise ratios, while differential responding was only evident during sustained response intervals. In these later time intervals, enhanced disruption of the ssVEP signal suggests interference by a continuously changing video stream which is enhanced as a function of motivational relevance, i.e. the CTX+ stream (Campagnoli et al., 2019). These findings contribute to our understanding of the perceptional processing of more ecologically valid context stimuli and its modulation during situations of potential threat.

AUTHOR CONTRIBUTIONS

Yannik Stegmann: Conceptualization; data curation; formal analysis; investigation; methodology; project administration; resources; software; visualization; writing – original draft; writing – review and editing. **Marta Andreatta:** Formal analysis; methodology; visualization; writing – review and editing. **Paul Pauli:** Conceptualization; funding acquisition; methodology; project administration; resources; supervision; writing – review and editing. **Andreas Keil:** Resources; software; supervision; writing – review and editing. **Matthias Wieser:** Conceptualization; formal analysis; funding acquisition; methodology; project administration; software; supervision; validation; writing – review and editing.

DATA AVAILABILITY STATEMENT

All data and code are openly available at https://osf.io/azu6h/.

ORCID

Yannik Stegmann https://orcid.org/0000-0002-0933-8492
Marta Andreatta https://orcid.org/0000-0002-1217-8266
Andreas Keil https://orcid.org/0000-0002-4064-1924
Matthias J. Wieser https://orcid.org/0000-0002-0429-1541

REFERENCES

American Psychiatric Association. (2013). *Diagnostic and statistical manual of mental disorders (DSM-5)*. American Psychiatric Pub.

Andreatta, M., Glotzbach-Schoon, E., Muhlberger, A., Schulz, S. M., Wiemer, J., & Pauli, P. (2015). Initial and sustained brain responses to contextual conditioned anxiety in humans. *Cortex*, *63*, 352–363. https://doi.org/10.1016/j.cortex.2014.09.014

Andreatta, M., Neueder, D., Herzog, K., Genheimer, H., Schiele, M. A., Deckert, J., Domschke, K., Reif, A., Wieser, M. J., & Pauli, P. (2020). Generalization of conditioned contextual anxiety and the modulatory effects of anxiety sensitivity. *Neurotherapeutics*, *17*, 1239–1252. https://doi.org/10.1007/s13311-020-00831-8

Andreatta, M., & Pauli, P. (2021). Contextual modulation of conditioned responses in humans: A review on virtual reality studies. *Clinical Psychology Review*, *90*, 102095. https://doi.org/10.1016/j.cpr.2021.102095

Barry-Anwar, R., Hadley, H., Conte, S., Keil, A., & Scott, L. S. (2018). The developmental time course and topographic distribution of individual-level monkey face discrimination in the infant brain. *Neuropsychologia*, *108*, 25–31. https://doi.org/10.1016/j.neuropsychologia.2017.11.019

Bekhtereva, V., Pritschmann, R., Keil, A., & Müller, M. M. (2018). The neural signature of extracting emotional content from rapid visual streams at multiple presentation rates: A cross-laboratory study. *Psychophysiology*, *55*(12), e13222. https://doi.org/10.1111/psyp.13222

Boucsein, W., Fowles, D. C., Grimnes, S., Ben-Shakhar, G., roth, W. T., Dawson, M. E., Filion, D. L., & Society for Psychophysiological Research Ad Hoc Committee on Electrodermal Measures. (2012). Publication recommendations for electrodermal

measurements. *Psychophysiology*, *49*(8), 1017–1034. https://doi.org/10.1111/j.1469-8986.2012.01384.x

Bublatzky, F., Gerdes, A. B., & Alpers, G. W. (2014). The persistence of socially instructed threat: Two threat-of-shock studies. *Psychophysiology*, *51*(10), 1005–1014. https://doi.org/10.1111/psyp.12251

Campagnoli, R. R., Wieser, M. J., Gruss, L. F., Boylan, M. R., McTeague, L. M., & Keil, A. (2019). How the visual brain detects emotional changes in facial expressions: Evidence from driven and intrinsic brain oscillations. *Cortex*, *111*, 35–50. https://doi.org/10.1016/j.cortex.2018.10.006

Davis, M., Walker, D. L., Miles, L., & Grillon, C. (2010). Phasic vs sustained fear in rats and humans: Role of the extended amygdala in fear vs anxiety. *Neuropsychopharmacology*, *35*(1), 105–135. https://doi.org/10.1038/npp.2009.109

Fanselow, M. S. (1994). Neural organization of the defensive behavior system responsible for fear. *Psychonomic Bulletin & Review*, *1*(4), 429–438. https://doi.org/10.3758/BF03210947

Genheimer, H., Andreatta, M., & Pauli, P. (2020). Conjunctive and elemental representations of a context in humans. *Journal of Cognitive Neuroscience*, *32*(7), 1394–1406. https://doi.org/10.1162/jocn_a_01559

Glotzbach, E., Ewald, H., Andreatta, M., Pauli, P., & Muhlberger, A. (2012). Contextual fear conditioning predicts subsequent avoidance behaviour in a virtual reality environment. *Cognition and Emotion*, *26*(7), 1256–1272. https://doi.org/10.1080/02699931.2012.656581

Glotzbach-Schoon, E., Andreatta, M., Mühlberger, A., & Pauli, P. (2013). Context conditioning in virtual reality as a model for pathological anxiety. *e-Neuroforum*, *19*, 63–70.

Glotzbach-Schoon, E., Tadda, R., Andreatta, M., Troger, C., Ewald, H., Grillon, C., Pauli, P., & Muhlberger, A. (2013). Enhanced discrimination between threatening and safe contexts in high-anxious individuals. *Biological Psychology*, *93*(1), 159–166. https://doi.org/10.1016/j.biopsycho.2013.01.011

Grillon, C., Baas, J. M., Cornwell, B., & Johnson, L. (2006). Context conditioning and behavioral avoidance in a virtual reality environment: Effect of predictability. *Biological Psychiatry*, *60*(7), 752–759. https://doi.org/10.1016/j.biopsych.2006.03.072

Grillon, C., Baas, J. P., Lissek, S., Smith, K., & Milstein, J. (2004). Anxious responses to predictable and unpredictable aversive events. *Behavioral Neuroscience*, *118*(5), 916–924. https://doi.org/10.1037/0735-7044.118.5.916

Haaker, J., Maren, S., Andreatta, M., Merz, C. J., Richter, J., Richter, S. H., Meir Drexler, S., Lange, M. D., Jüngling, K., Nees, F., Seidenbecher, T., Fullana, M. A., Wotjak, C. T., & Lonsdorf, T. B. (2019). Making translation work: Harmonizing cross-species methodology in the behavioural neuroscience of Pavlovian fear conditioning. *Neuroscience & Biobehavioral Reviews*, *107*, 329–345. https://doi.org/10.1016/j.neubiorev.2019.09.020

Junghofer, M., Elbert, T., Tucker, D. M., & Rockstroh, B. (2000). Statistical control of artifacts in dense array EEG/MEG studies. *Psychophysiology*, *37*(4), 523–532. https://doi.org/10.1111/1469-8986.3740523

Kastner, A. K., Pauli, P., & Wieser, M. J. (2015). Sustained attention in context conditioning: Evidence from steady-state VEPs. *International Journal of Psychophysiology*, *98*(3 Pt 2), 546–556. https://doi.org/10.1016/j.ijpsycho.2015.03.005

Kastner-Dorn, A. K., Andreatta, M., Pauli, P., & Wieser, M. J. (2018). Hypervigilance during anxiety and selective attention during fear: Using steady-state visual evoked potentials (ssVEPs) to disentangle attention mechanisms during predictable and unpredictable threat. *Cortex*, *106*, 120–131. https://doi.org/10.1016/j.cortex.2018.05.008

Keil, A., Debener, S., Gratton, G., Junghofer, M., Kappenman, E. S., Luck, S. J., Luu, P., Miller, G. A., & Yee, C. M. (2014). Committee report: Publication guidelines and recommendations for studies using electroencephalography and magnetoencephalography. *Psychophysiology*, *51*(1), 1–21. https://doi.org/10.1111/psyp.12147

Keil, A., Miskovic, V., Gray, M. J., & Martinovic, J. (2013). Luminance, but not chromatic visual pathways mediate amplification of conditioned danger signals in human visual cortex. *The European Journal of Neuroscience*, *38*(9), 3356–3362. https://doi.org/10.1111/ejn.12316

Klinke, C. M., Fiedler, D., Lange, M. D., & Andreatta, M. (2020). Evidence for impaired extinction learning in humans after distal stress exposure. *Neurobiology of Learning and Memory*, *167*, 107127. https://doi.org/10.1016/j.nlm.2019.107127

LaBar, K. S., & Phelps, E. A. (2005). Reinstatement of conditioned fear in humans is context dependent and impaired in amnesia. *Behavioral Neuroscience*, *119*(3), 677–686. https://doi.org/10.1037/0735-7044.119.3.677

Lang, P. J., Davis, M., & Ohman, A. (2000). Fear and anxiety: Animal models and human cognitive psychophysiology. *Journal of Affective Disorders*, *61*(3), 137–159. https://doi.org/10.1016/s0165-0327(00)00343-8

Lang, S., Kroll, A., Lipinski, S. J., Wessa, M., Ridder, S., Christmann, C., Schad, L. R., & Flor, H. (2009). Context conditioning and extinction in humans: Differential contribution of the hippocampus, amygdala and prefrontal cortex. *The European Journal of Neuroscience*, *29*(4), 823–832. https://doi.org/10.1111/j.1460-9568.2009.06624.x

Maren, S., Phan, K. L., & Liberzon, I. (2013). The contextual brain: Implications for fear conditioning, extinction and psychopathology [review]. *Nature Reviews. Neuroscience*, *14*(6), 417–428. https://doi.org/10.1038/nrn3492

McTeague, L. M., Gruss, L. F., & Keil, A. (2015). Aversive learning shapes neuronal orientation tuning in human visual cortex [article]. *Nature Communications*, *6*, 7823. https://doi.org/10.1038/ncomms8823

Miskovic, V., & Keil, A. (2012). Acquired fears reflected in cortical sensory processing: A review of electrophysiological studies of human classical conditioning. *Psychophysiology*, *49*(9), 1230–1241. https://doi.org/10.1111/j.1469-8986.2012.01398.x

Moratti, S., Clementz, B. A., Gao, Y., Ortiz, T., & Keil, A. (2007). Neural mechanisms of evoked oscillations: Stability and interaction with transient events. *Human Brain Mapping*, *28*(12), 1318–1333. https://doi.org/10.1002/hbm.20342

Muller, M. M., Andersen, S. K., & Keil, A. (2008). Time course of competition for visual processing resources between emotional pictures and foreground task. *Cerebral Cortex*, *18*(8), 1892–1899. https://doi.org/10.1093/cercor/bhm215

Norcia, A. M., Appelbaum, L. G., Ales, J. M., Cottereau, B. R., & Rossion, B. (2015). The steady-state visual evoked potential in vision research: A review. *Journal of Vision*, *15*(6), 4. https://doi.org/10.1167/15.6.4

Öhman, A., Flykt, A., & Esteves, F. (2001). Emotion drives attention: Detecting the snake in the grass. *Journal of Experimental Psychology: General*, *130*(3), 466–478. https://doi.org/10.1037/0096-3445.130.3.466

Peyk, P., De Cesarei, A., & Junghofer, M. (2011). ElectroMagnetoEncephalography software: Overview and integration with other EEG/MEG toolboxes. *Computational Intelligence and Neuroscience*, *2011*, 861705. https://doi.org/10.1155/2011/861705

Richards, H. J., Benson, V., Donnelly, N., & Hadwin, J. A. (2014). Exploring the function of selective attention and hypervigilance for threat in anxiety. *Clinical Psychology Review*, *34*(1), 1–13. https://doi.org/10.1016/j.cpr.2013.10.006

Riels, K. M., Rocha, H. A., & Keil, A. (2020). No intermodal interference effects of threatening information during concurrent audiovisual stimulation. *Neuropsychologia*, *136*, 107283. https://doi.org/10.1016/j.neuropsychologia.2019.107283

Stegmann, Y., Ahrens, L. M., Pauli, P., Keil, A., & Wieser, M. J. (2020). Social aversive generalization learning sharpens the tuning of visuocortical neurons to facial identity cues. *eLife*, *9*, e55204. https://doi.org/10.7554/eLife.55204

Stegmann, Y., Reicherts, P., Andreatta, M., Pauli, P., & Wieser, M. J. (2019). The effect of trait anxiety on attentional mechanisms in combined context and cue conditioning and extinction learning. *Scientific Reports*, *9*(1), 8855. https://doi.org/10.1038/s41598-019-45239-3

Stolz, C., Endres, D., & Mueller, E. M. (2019). Threat-conditioned contexts modulate the late positive potential to faces—A mobile EEG/virtual reality study. *Psychophysiology*, *56*(4), e13308. https://doi.org/10.1111/psyp.13308

Stout, D. M., Glenn, D. E., Acheson, D. T., Simmons, A. N., & Risbrough, V. B. (2019). Characterizing the neural circuitry associated with configural threat learning. *Brain Research*, *1719*, 225–234. https://doi.org/10.1016/j.brainres.2019.06.003

Stout, D. M., Glenn, D. E., Acheson, D. T., Spadoni, A. D., Risbrough, V. B., & Simmons, A. N. (2018). Neural measures associated with configural threat acquisition. *Neurobiology of Learning and Memory*, *150*, 99–106. https://doi.org/10.1016/j.nlm.2018.03.012

Vansteenwegen, D., Iberico, C., Vervliet, B., Marescau, V., & Hermans, D. (2008). Contextual fear induced by unpredictability in a human fear conditioning preparation is related to the chronic expectation of a threatening US. *Biological Psychology*, *77*(1), 39–46. https://doi.org/10.1016/j.biopsycho.2007.08.012

Wieser, M. J., Flaisch, T., & Pauli, P. (2014). Raised middle-finger: Electrocortical correlates of social conditioning with nonverbal affective gestures. *PLoS One*, *9*(7), e102937. https://doi.org/10.1371/journal.pone.0102937

Wieser, M. J., & Keil, A. (2011). Temporal trade-off effects in sustained attention: Dynamics in visual cortex predict the target detection performance during distraction. *Journal of Neuroscience*, *31*(21), 7784–7790. https://doi.org/10.1523/JNEUROSCI.5632-10.2011

Wieser, M. J., & Keil, A. (2014). Fearful faces heighten the cortical representation of contextual threat. *NeuroImage*, *86*, 317–325. https://doi.org/10.1016/j.neuroimage.2013.10.008

Wieser, M. J., Reicherts, P., Juravle, G., & von Leupoldt, A. (2016). Attention mechanisms during predictable and unpredictable threat - a steady-state visual evoked potential approach. *NeuroImage*, *139*, 167–175. https://doi.org/10.1016/j.neuroimage.2016.06.026